14

Collapse Behavior of Moderately Thick Tubes Pressurized from Outside

Leone Corradi, Antonio Cammi and Lelio Luzzi
Politecnico di Milano - Department of Energy
Enrico Fermi Center for Nuclear Studies (CeSNEF)
Italy

1. Introduction

This study originated from a specific problem that arose in conjunction with the IRIS (International Reactor Innovative and Secure) project (Carelli et al., 2004; Carelli, 2009). IRIS adopts an integrated primary system reactor (IPSR) configuration with all the primary loop components of a classical Pressurized Water Reactor (PWR) contained inside the vessel (Fig. 1). Among the reactor core internals are the steam generator (SG) units (Cinotti et al., 2002) with the primary fluid flowing outside the tube bundles and subjecting them to significant external pressure. In this situation buckling affects the tube collapse modality and codes become extremely conservative, to the point that up to five years ago design procedures based on the *ASME Boiler & Pressure Vessel* code (Section III) required an external diameter to thickness ratio (D/t) less than 8.5, leading to an increased thermal resistance in the heat exchange process between primary and secondary fluids, with detrimental consequences on the dimensioning of the heat transfer surface. A reduction in the tube thickness would allow the reduction of the overall heat transfer surface needed to exchange the same amount of power, with consequent saving on tube lengths and/or number of tubes. On the other hand, if the design of the steam generator units is not modified, an increase in the exchanged thermal power and a consequent up rating of the reactor can be obtained.
Besides IRIS, other recent proposals for next generation power plants based on PWR technology consider an IPSR design (Ingersoll, 2009; Karahan, 2010; Ninokata, 2006). Such integrated design is particularly suitable for small sized units, i.e., reactors with a power less than 300 MWe following the IAEA's definition (IAEA, 2007). A significant number of small sized PWR IPSRs is currently under development (e.g., RITM-200, ABV, CAREM, SMART, MRX, NHR-200, Westinghouse SMR, mPower, NuScale, see http://www.world-nuclear.org/info/inf33.html). Packing all the PWR primary components into the reactor pressure vessel (RPV) (Fig. 2) offers several advantages (Ingersoll, 2009): (i) all large coolant pipes are eliminated (only small feed water and steam outlet pipes penetrate the vessel wall); (ii) the total inventory of primary coolant is much larger than for an external loop PWR (this feature increases the heat capacity and thermal inertia of the system and hence yields a much slower response to core heat-up transients); (iii) typically the heat exchangers are placed above the core creating a relatively tall system that facilitates more effective natural circulation of the primary coolant in the case of a coolant pump failure; (iv) the vessel accommodates a relatively large pressurizer volume that provides better control

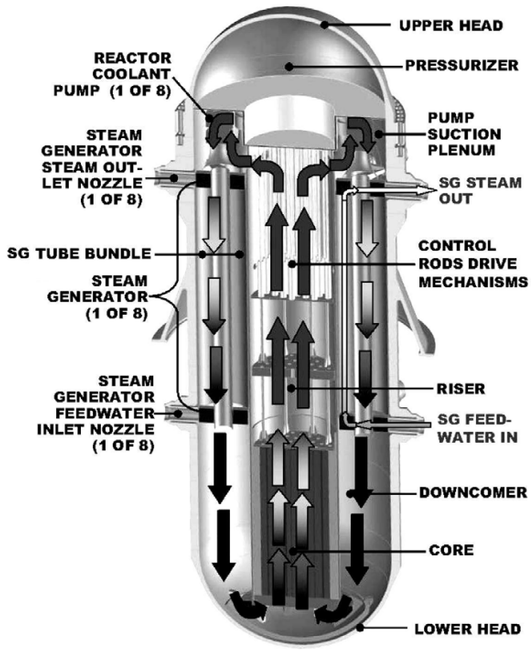

Fig. 1. IRIS reactor pressure vessel module (Reproduced from (Luzzi & Di Marcello, 2011))

of under/overpressure transients; and (v) the extended riser area provides the possibility for internal placement of the control rod drive mechanisms, thus avoiding the potentially serious accident scenario represented by the rod ejection.

All these solutions entail the presence of tubes or pipes pressurized from outside and, as for IRIS, their sizing has to face the severity of the code. It was felt that ASME code requirements were exceedingly conservative and both numerical (Corradi et al., 2009) and experimental (Lo Frano & Forasassi, 2009) investigations were performed to assess the collapse pressure of the tubes. The first results obtained within this framework contributed to the approval of Section III Code Case N-759 (ASME, 2007), which permits considerable thickness saving. From a regulation point of view the problem of excessive thickness was overcome, but the question of the collapse behavior of tubes in this thickness range remains open. These tubes are thicker not only than the very thin shells typical of aerospace applications, but also than the moderately thin tubes employed in oil industry as pipes or casings. On the other hand, they are not as thick as those that are encountered in high pressure technology and their behavior has been the object of a limited amount of study so far.

Very thin shells fail because of elastic buckling and very thick tubes because of plastic collapse, so that their ultimate pressures can be established on theoretical ground, by exploiting well established results (Budiansky, 1974; Mendelson, 1968). In the intermediate range, on the contrary, plasticity and buckling interact and, in principle, the strength of the tube can only be assessed numerically. Attempts at reproducing numerical results with empirical design formulas were also made at the end of the last century (e.g., (Haagsma & Schaap,

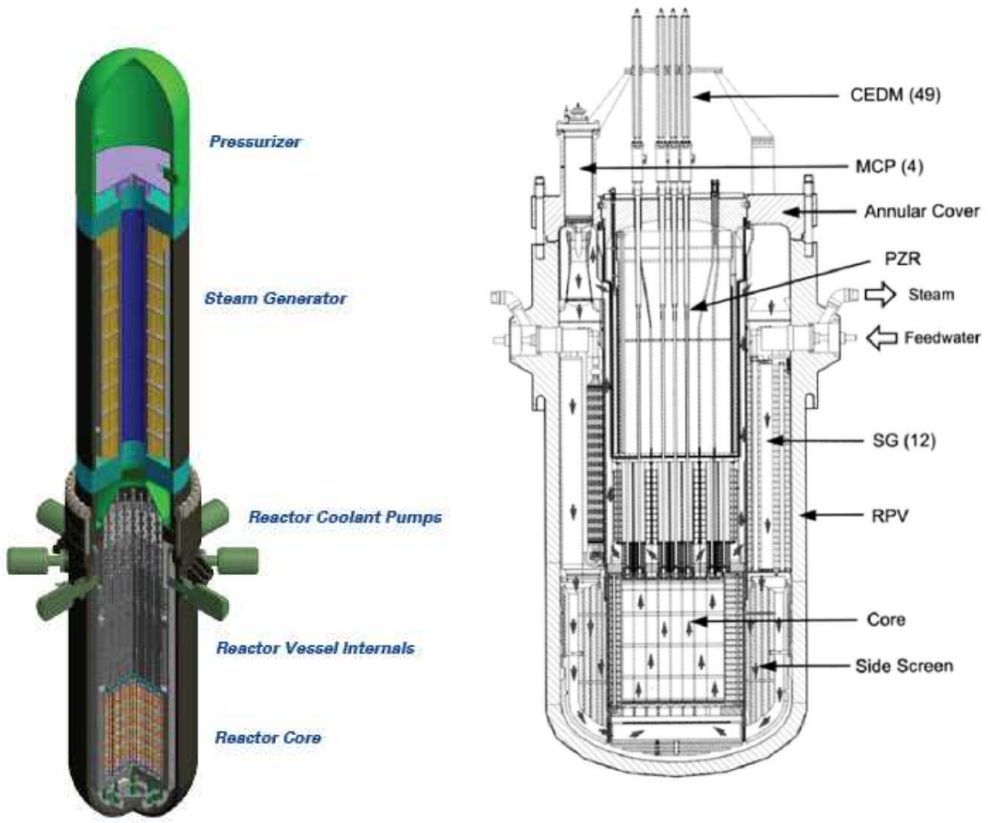

(a) (b)

Fig. 2. Integrated primary system reactors of small size. (a) Westinghouse SMR-200 MWe (Small Modular Reactor); (b) SMART-90 MWe (System Integrated Modular Advanced Reactor). Reproduced from http://www.westinghousenuclear.com/smr/fact_sheet.pdf and from (Ninokata, 2006), respectively

1981; Tamano et al., 1985; Yeh & Kyriakides, 1988)): such results are adequate in the range of interest for oil industry, but become questionable for the thicker tubes required by the nuclear applications mentioned above. In this range, collapse is dominated by yielding, but interaction with buckling is still significant and reduces the pressure bearing capacity by an amount that cannot be disregarded when safety is of primary concern.

The problem is similar to that of beam columns of intermediate slenderness, which also fail because of interaction between yielding and buckling and that have been studied in detail. A simple predictive formula was proposed in this context, which turns out to be reasonably accurate for any slenderness and several code recommendations are based on it (e.g., (EUROCODE 3, 1993)). An attempt at adapting such formula to the case of tubes was made in (Corradi et al., 2008), but a direct modification was successful only in the medium thin tube range, where the formula appears as a feasible alternative to other proposals. With increasing thickness the formula becomes conservative and only provides a, often coarse, lower bound to the collapse pressure. A correction was proposed which, however, is to a large extent empirical and based on fitting of numerical results.

In this study a different proposal is advanced, which is felt to better embody the physical nature of the phenomenological behavior. Comparison shows that tubes behave essentially as columns for $D/t \geq 25-30$, but differences make their appearance and grow up to significant values as this ratio diminishes. One reason is of geometric nature: the curvature of the tube wall increases with diminishing D/t ratio and the analogy with a straight column no longer applies. Another source of discrepancy is the stress redistribution capability that thick tubes, in contrast to columns, possess and can exploit with significant benefit. This aspect is not purely geometric: stress redistribution *capability* is still function of thickness, but the possibility of exploiting it is influenced by material properties as well. By properly interpreting these aspects, a formula is obtained that appears reasonably simple and accurate. In addition, it is felt that it provides a deeper understanding on the collapse behavior of cylindrical shells in a thickness range so far overlooked.
A comment on terminology is in order. Labels like "thick" or "thin" when applied to tubes are to some extent ambiguous, since they are used in a different sense in different contexts. A pipeline in deep sea water would be considered as a thick tube by an aerospace engineer and as thin one by high pressure technology people. Often, the term "thin tube" is used when thin shell assumptions, which consider stresses to be constant over the thickness, apply, but this definition also becomes questionable outside the elastic range. In this study, reference is made to the failure modality. A tube is called *thin* if it fails because of elastic buckling and *thick* when only plastic collapse is relevant. In the intermediate region the two failure modalities interact, with different weight for different slenderness. In *moderately thin* (or *medium thin*) tubes, buckling is the critical phenomenon even if plasticity plays some role; similarly, in *moderately thick* tubes failure is dominated by yielding, but interaction with buckling has non negligible effects. The separation line is not very sharp (in oil industry applications, for instance, the two phenomena have comparable weight), but the tubes of prominent interest in this study definitively belong to the *moderately thick* range.

2. Collapse of cylindrical shells pressurized from outside

2.1 Basic theoretical results

Consider a cylindrical shell of nominal circular shape, with outer diameter D and wall thickness t, subjected to an external pressure q. The shell is long enough for end effects to be disregarded. The material is isotropic, elastic-perfectly plastic and governed by von Mises' criterion. E and ν are its elastic constants (Young modulus and Poisson ratio, respectively) and σ_0 denotes the tensile yield strength.
In the theoretical situation of a perfect tube, the limit pressure is given by the smallest among the following values

$$\textit{Elastic buckling pressure} \qquad q_E = 2\frac{E}{1-\nu^2}\frac{1}{\frac{D}{t}\left(\frac{D}{t}-1\right)^2} \tag{1a}$$

$$\textit{Plastic limit pressure} \qquad q_0 = 2\sigma_0\frac{t}{D}\left(1+\frac{1}{2}\frac{t}{D}\right) \tag{1b}$$

The first expression is well known (Timoshenko & Gere, 1961), while equation (1b) was established in (Corradi et al., 2005) and is a very good approximation to the exact value for $D/t > 6$.

Equations (1) apply to possibly thick tubes, which demand that stress variation over the thickness be considered. Nevertheless, the average value S of the hoop stress σ_ϑ is a meaningful piece of information. Its value is dictated by equilibrium only and reads

$$S = \frac{1}{2} q \frac{D}{t} \tag{2}$$

For thick cylinders, peak stresses may exceed significantly the value (2), which is simply an alternative, often convenient, way to refer to pressure. In particular, the theoretical limits (1) may be replaced by the expressions

$$S_E = \frac{E}{1-\nu^2} \frac{1}{\left(\frac{D}{t}-1\right)^2} \qquad S_0 = \sigma_0 \left(1 + \frac{1}{2}\frac{t}{D}\right) \tag{3}$$

which are obtained by substituting in equation (2) either of the values (1) for q.
As the thickness decreases, local values approach their average and equation (2) becomes meaningful as a stress intensity measure for sufficiently thin tubes, which are usually studied by assuming $\sigma_\vartheta \approx S$. Also, the difference between the outer face of the tube, where the pressure acts, and the middle surface, where the resultant of hoop stresses is applied, is ignored. Within this framework, equations (1) become

$$\textit{Elastic buckling pressure} \qquad p_E = 2\frac{E}{1-\nu^2}\left(\frac{t}{D}\right)^3 \tag{4a}$$

$$\textit{Plastic limit pressure} \qquad p_0 = 2\sigma_0 \frac{t}{D} \tag{4b}$$

or, in terms of average hoop stress

$$F_E = \frac{E}{1-\nu^2}\left(\frac{t}{D}\right)^2 \qquad F_0 = \sigma_0 \tag{5}$$

Here (and in the sequel) p is used instead of q and F instead of S when computations are based on thin shell assumptions.
In the theoretical situation, the two critical phenomena of elastic buckling and plastic collapse are independent from each other. The quantity

$$\Lambda = \sqrt{\frac{q_0}{q_E}} = \sqrt{\frac{1}{\kappa}\left(\frac{D^2}{t^2} - \frac{3}{2}\frac{D}{t} + \frac{1}{2}\frac{t}{D}\right)} \tag{6}$$

or, if thin shell approximation is adopted

$$\Lambda = \sqrt{\frac{p_0}{p_E}} = \frac{1}{\sqrt{\kappa}}\frac{D}{t} \tag{7}$$

is known as *slenderness ratio*. The parameter

$$\kappa = \frac{1}{1-\nu^2}\frac{E}{\sigma_0} \tag{8}$$

is a dimensionless material property. $\Lambda = 1$ is the *transition value*, separating the range of comparatively thin tubes ($\Lambda > 1$, $q_E < q_0$), theoretically failing because of elastic buckling, from that of comparatively thick ones ($\Lambda < 1$, $q_0 < q_E$), when the critical situation is plastic collapse. Fig. 3 depicts schematically the two failure modalities.

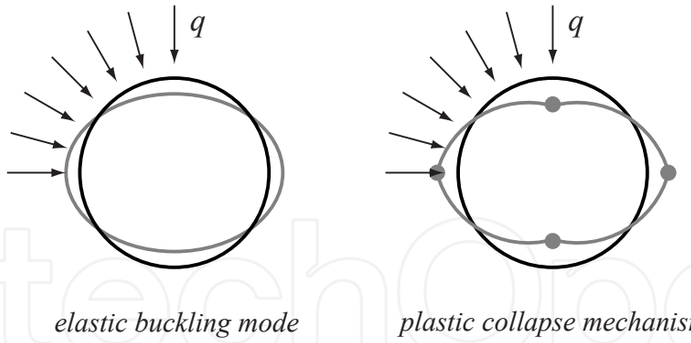

Fig. 3. Failure modalities for a long tube

2.2 Effects of imperfections

The situation above is "theoretical" in that it refers to the ideal case of a *perfect* tube. A real tube is unavoidably affected by imperfections, which introduce an interaction between plasticity and instability. As a consequence, the ultimate pressure is lower than the theoretical value. Fig. 4 depicts some aspects of the solution of a tube with an initial out of roundness (*ovality*): the pressure-displacement curve grows up to a maximum value, corresponding to failure, and then decreases; at the maximum, the tube is only partially yielded, i.e., plastic zones (in color) nowhere spread across the entire tube thickness (Fig. 4a). The "four hinge" mechanism is is attained in the post-collapse portion of the curve only (Fig. 4b). Failure occurs because of *buckling of the partially yielded tube*: even if not forming a mechanism, plastic zones reduce the tube stiffness and make the buckling load diminish. Failure corresponds to the elastic buckling of a tube of variable thickness, consisting of the current elastic portion.

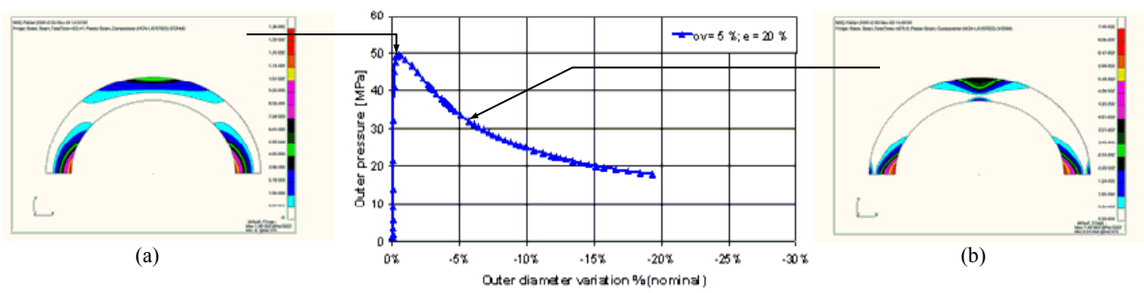

Fig. 4. Response of an initially oval tube. (a) plastic zones at failure; (b) four hinge mechanism in the post-collapse phase

To compute the failure pressure, complete elastic-plastic, large displacement analyses up to collapse are required, explicitly accounting for different kinds of possible imperfections. A systematic study was undertaken at the Politecnico di Milano and results are summarized in (Corradi et al., 2009; Luzzi & Di Marcello, 2011). Imperfections of both geometrical (initial out of roundness, non uniform thickness) and mechanical (initial stresses) nature were considered. As in a sense expected, it was found that all of them have similar consequences, causing a significant decay of the failure pressure with respect to the theoretical one for slenderness ratios close the transition value, with interaction effects diminishing as Λ departs from one in either direction. In any case, some decay was experienced in the entire range $0.2 \leq \Lambda \leq 5$, covering all situations of practical interest, except possibly high pressure technology or

aerospace engineering. The slenderness ratio of tubes for the aforesaid nuclear applications is low, but not enough to disregard the effects of interaction with instability: the IRIS steam generator tubes bundles, if sized according to Code Case N-759, correspond to $\Lambda \approx 0.4$.
When the study was started, Code Case N-759 was not available and ASME Section III rules required an external diameter to thickness ratio $D/t = 8.27$ ($\Lambda \approx 0.25$). Such a design is surprisingly severe and it was felt that the code assumed an *a-priori* conservative attitude for tubes belonging to a range scarcely studied both from the numerical and the experimental points of view, reflecting a substantial lack of knowledge on the phenomena involved. The numerical campaign was intended as a first step toward the definition of a suitable failure pressure, a reliable reference value permitting the derivation of an allowable working pressure through the use of a proper safety factor (Corradi et al., 2008). Computations had to include imperfections (one drawback of ASME III rules was that imperfections were not explicitly considered) but, since the effects of all of them were found to be similar, only the most significant was considered. This was identified with an initial out of roundness, or *ovality*, defined by the dimensionless parameter

$$W = \frac{D_{\max} - D_{\min}}{D} \tag{9}$$

where $D_{\max}$ and $D_{\min}$ are the maximum and minimum diameters of the ellipsis portraying the external surface of the tube (see Fig. 8a in the subsequent section) and D is their average value (nominal external diameter). To the failure pressure q_C computed in this way (a reasonable choice for the reference value) a safety factor is applied so as to reproduce ASME Section III sizing for medium thin tubes, a well known and well explored range, in which the code can be assumed to consider the proper safety margin (see (Corradi et al., 2008) for details). If the same factor is applied to thicker tubes as well, significant thickness saving is achieved without jeopardizing safety.
The requirement that the reference pressure be computed numerically makes the procedure cumbersome and an attempt at reproducing numerical results with an empirical formula was made (Corradi et al., 2008). The formula is adequate for practical purposes, but the approach is not completely satisfactory for a number of reasons: (i) the formula is involved and a simpler expression is desirable; (ii) its empirical nature does not help the understanding of the mechanical aspects of the tube behavior, and (iii) the formula is not equally accurate for all materials. Its coefficients were determined by considering the material envisaged for the IRIS SG tube bundles, i.e. Nickel-Chromium-Iron alloy N06690 (INCONEL 690) and the formula is fairly precise for $700 \leq \kappa \leq 1100$, where κ is defined by equation (8). Some materials, however, either because of high tensile yield strength σ_0 or low Young modulus E, have values of κ significantly below the lower limit; in these instances, the formula entails errors up to 10%, even if always on the safe side. Table 1 lists some of the materials investigated, with the properties employed in (Corradi et al., 2008) for computations and that will be used in this study as well. Trouble was experienced with aluminum and titanium alloys.

3. Interaction domains

3.1 Preliminary: load bearing capacity of struts

The proposal advanced in this study originates from the approach used to evaluate the collapse load of compressed columns, which is briefly outlined to introduce the procedure.
Consider the strut in compression illustrated in figure 5a. Its center line has an initially sinusoidal shape of amplitude U. The critical section, obviously, is the central one, where

material	E (GPa)	σ_0 (MPa)	ν	κ	$\left(\frac{D}{t}\right)_{\Lambda=0.2}$
stainless steel UNS S31600	200	200	0.31	1106	7.44
nickel-chromium-iron alloy N06690	183	240	0.29	832	6.56
aluminum alloy UNS A96061	70	240	0.35	332	4.46
titanium alloy UNS R56400	110	830	0.34	150	3.28

Table 1. Material properties for the considered materials

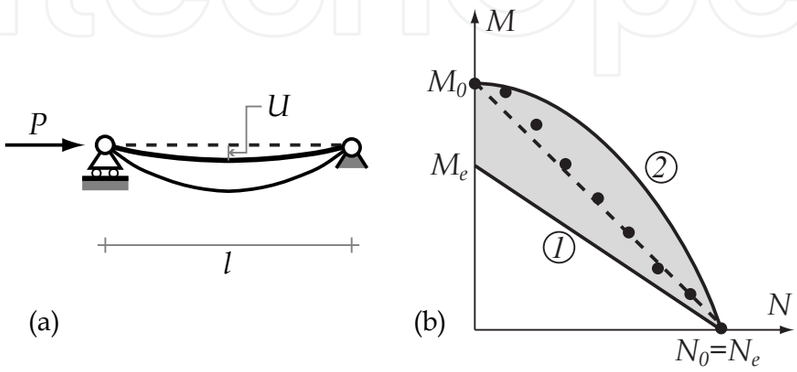

Fig. 5. Compressed column with initial imperfection

the axial force is $N = P$ (compression positive) and the bending moment M is expressed as

$$M = PU\frac{1}{1-\frac{P}{P_E}} \tag{10}$$

where P_E is the Euler buckling load ($P_E = \pi^2 EI/l^2$) and $1/\left(1 - P/P_E\right)$ the *magnification factor*. Equation (10) is exact in the elastic range since the initial imperfection has the same shape as the buckling mode (Timoshenko & Gere, 1961).
The behavior of the cross section is subsumed by the *interaction diagrams* in figure 5b. Line 1 is the *elastic limit* and for $N - M$ values on it one fiber is about to yield; line 2 is the *limit curve*, bounding the domain of $N - M$ combinations that can be borne. The gray zone is the elastic plastic region, corresponding to partially yielded sections. N_e and M_e are the values that individually bring the section at the onset of yielding, N_0 and M_0 the corresponding values exhausting the sectional bearing capacity. Obviously, it is $N_e = N_0$, since in pure compression stresses are uniform. The elastic limit is given by

$$\frac{N}{N_e} + \frac{M}{M_e} = 1 \tag{11a}$$

while the equation of the limit curve depends on the sectional shape. For rectangular cross sections one has

$$\left(\frac{N}{N_0}\right)^2 + \frac{M}{M_0} = 1 \tag{11b}$$

with $M_0 = \frac{3}{2}M_e$.

By substituting equation (10) for M into (11a), a quadratic equation for P is obtained, which is easily solved to give the load P_{el} exhausting the elastic resources of the strut and bounding from below its load bearing capacity P_C. The same procedure applied with (11b) replacing (11a) provides an *upper bound* to P_C. In fact, at collapse some fibers of the central section are still elastic (Fig. 6) and the corresponding $N - M$ point is *inside* the limit domain. Some collapse situations are indicated by dots in figure 5b (the representation is qualitative, the location of the points being influenced to some extent by the strut slenderness). Observe also that the expression (10) for the maximum bending moment looses its validity outside the elastic range.

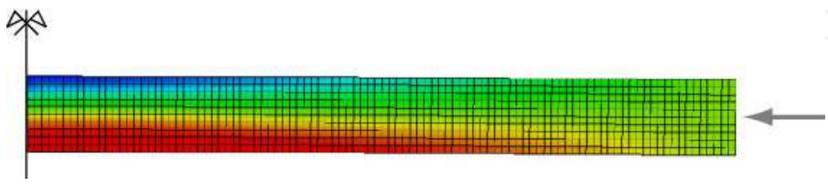

Fig. 6. Typical column at collapse: plastic strains develop in the red zone

A reasonable approximation to the collapse load is obtained by assuming that the $N - M$ points at collapse are located on the straight line

$$\frac{N}{N_0} + \frac{M}{M_0} = 1 \tag{12}$$

(dashed in figure 5b) and that the elastic relation (10) holds up to this point. One obtains

$$P_C = \frac{1}{2}\left(N_0 + P_E\left(1 + U\frac{N_0}{M_0}\right) - \sqrt{\left(N_0 + P_E\left(1 + U\frac{N_0}{M_0}\right)\right)^2 - 4N_0P_E}\right) \tag{13}$$

For rectangular $(b \times h)$ cross sections it is $N_0 = \sigma_0 bh$, $M_0 = \frac{1}{4}\sigma_0 bh^2$ and the column slenderness can be written as $\lambda = 2\sqrt{3}\frac{l}{h}$. By considering the slenderness ratio

$$\Lambda = \sqrt{\frac{N_0}{P_E}} = \frac{\lambda}{\lambda_0} \tag{14}$$

where

$$\lambda_0 = \pi\sqrt{\frac{E}{\sigma_0}} \tag{15}$$

is the *transition slenderness* (a material property) and by introducing the dimensionless imperfection measure

$$W = \frac{U}{l} \tag{16}$$

one can write equation (13) in the form

$$P_C = \frac{1}{2}\left(N_0 + P_E\left(1 + Z\right) - \sqrt{\left(N_0 + P_E\left(1 + Z\right)\right)^2 - 4N_0P_E}\right) \tag{17a}$$

with

$$Z = U\frac{N_0}{M_0} = \frac{2}{\sqrt{3}}\lambda_0 \Lambda W \tag{17b}$$

Equation (17) is a good approximation to the numerically computed failure load of compressed columns, as depicted in Fig. 7 where results for two materials with strongly different properties and a few initial imperfection magnitudes are compared. Several codes, including EUROCODE 3, base their recommendations on it (Dowling, 1990).

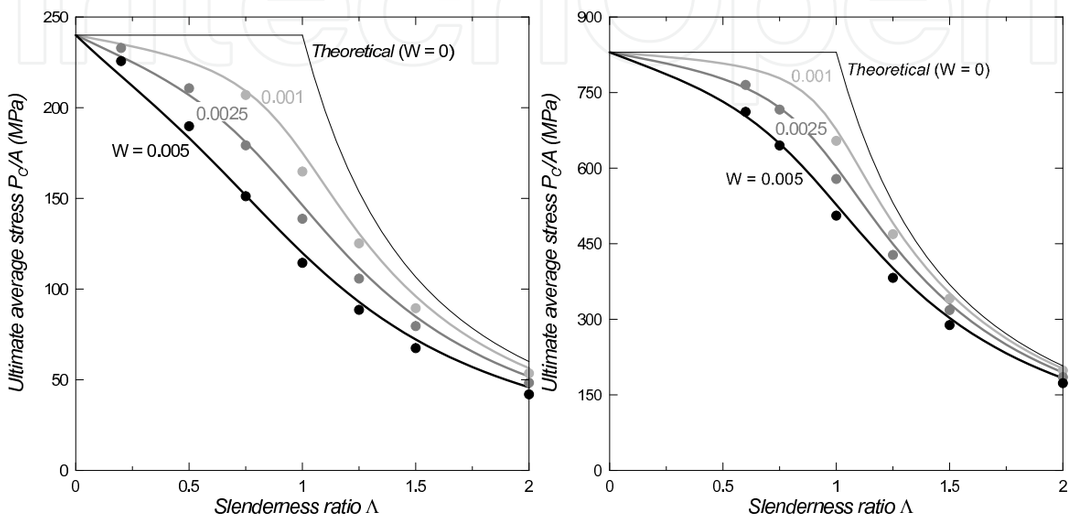

(a) INCONEL 690 ($\lambda_0 = 86.8$) (b) Titanium alloy ($\lambda_0 = 36.2$)

Fig. 7. Formula (17) vs computed results (dots). Λ defined by equation (14)

3.2 Interaction domain for an oval tube

Consider now a cylindrical shell with an initial imperfection controlled by W, equation (9), as illustrated in figure 8. Because of W, the external pressure q will cause, besides compressive hoop stresses, a bending moment with peak values given by the relation

$$M = M_I \frac{1}{1 - \frac{q}{q_E}} \tag{18a}$$

where

$$M_I = \frac{1}{8} q D^2 W \tag{18b}$$

is the value predicted within the small displacements framework (geometric linearity) and q_E is the Euler buckling pressure (1a). The expression (18) for M is exact in the elastic range if the initial imperfection has the same shape as the buckling mode (Timoshenko & Gere, 1961).
As for beam columns, the behavior of the tube wall can be interpreted on the basis of suitable interaction domains, with the external pressure q playing the role of the compression force and equation (18) replacing (10) to express the peak value of the bending moment. The domains are sketched in figure 8b: as in the equivalent picture for the strut, line 1 bounds the elastic

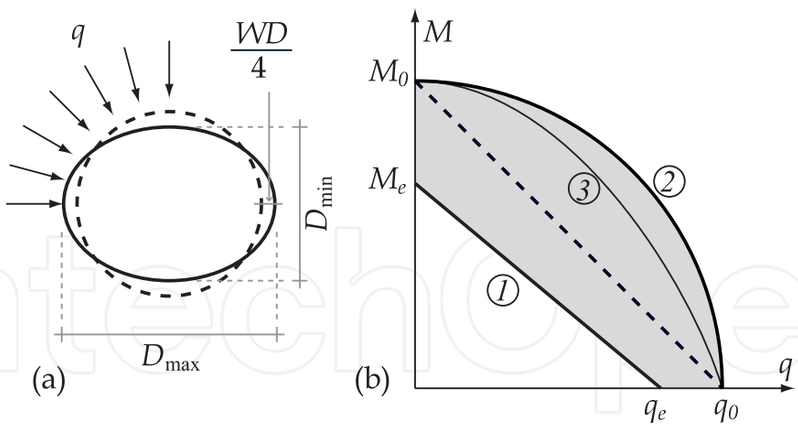

Fig. 8. Interaction domain for the tube cross section

region and line 2 is the limit curve. Reference values are assumed as follows (Corradi et al., 2008)

$$q_e = 2\sigma_0 \frac{t}{D}\left(1 - \frac{t}{D}\right) \qquad q_0 = 2\sigma_0 \frac{t}{D}\left(1 + \frac{1}{2}\frac{t}{D}\right) \tag{19a}$$

$$M_e = \frac{\sigma_0}{\sqrt{1-\nu+\nu^2}} \frac{\frac{1}{4}\left(b^2-a^2\right)^2 - a^2b^2\left(\ln\frac{b}{a}\right)^2}{2b^2\ln\frac{b}{a} - \left(b^2-a^2\right)} \qquad M_0 \approx \frac{\sigma_0 t^2}{2\sqrt{3}} \tag{19b}$$

where q_e, M_e and q_0, M_0 are the pressure and moment values that individually bring the tube at the onset of yielding and exhaust its load bearing capacity. $b = D/2$ and $a = b - t$ are the external and internal nominal radii, respectively.

The values above refer to materials governed by von Mises' criterion. Elastic stresses are computed from the well known plane solutions for a round cylinder under external pressure and for a curved beam subject to constant bending moments (Timoshenko & Goodier, 1951) and the values of q_e, M_e are obtained on this basis. q_0 is given by equation (1b), rewritten for completeness; the value $(19b)_2$ of M_0 actually refers to a straight beam and, for tubes thick enough to demand that curvature be considered, entails an error not completely negligible but acceptable: bending moments being caused by imperfections, only the portion of the domains close to the q axis is of interest.

The interaction domains for the tube and the strut of rectangular cross section exhibit some differences that become significant with increasing tube thickness. First of all, while the ratio M_0/M_e maintains more or less the value of 1.5, q_0 exceeds q_e by an amount that must be considered for $D/t < 25$. Moreover, in thick tubes the hoop stresses due to pressure are not uniform, which provides additional stress redistribution capabilities, so that the limit curve is expected to be external to that of the equivalent strut (the situation is sketched in figure 8b, where curve 3 (thinner) portrays the parabola (11b) with q replacing N). As a consequence, the region of partially yielded tubes (in gray), which contains the collapse situations, widens considerably, augmenting the uncertainties in estimating the failure pressure.

Nevertheless, the extension to tubes of the beam-column procedure is spontaneous and an attempt in this sense is made by introducing equation (18) for M in the linear expression

$$\frac{q}{q_0} + \frac{M}{M_0} = 1 \tag{20}$$

corresponding to the dashed segment in Fig. 8b. As for columns, a second order equation is obtained; its smallest root reads

$$q_C = \frac{1}{2}\left[q_0 + q_E\,(1+Z) - \sqrt{(q_0 + q_E\,(1+Z))^2 - 4q_0 q_E}\right] \tag{21a}$$

with

$$Z = \frac{\sqrt{3}}{2}\left(\frac{D}{t} + \frac{1}{2}\right) W \tag{21b}$$

The analogy with equation (17a) is immediately apparent.

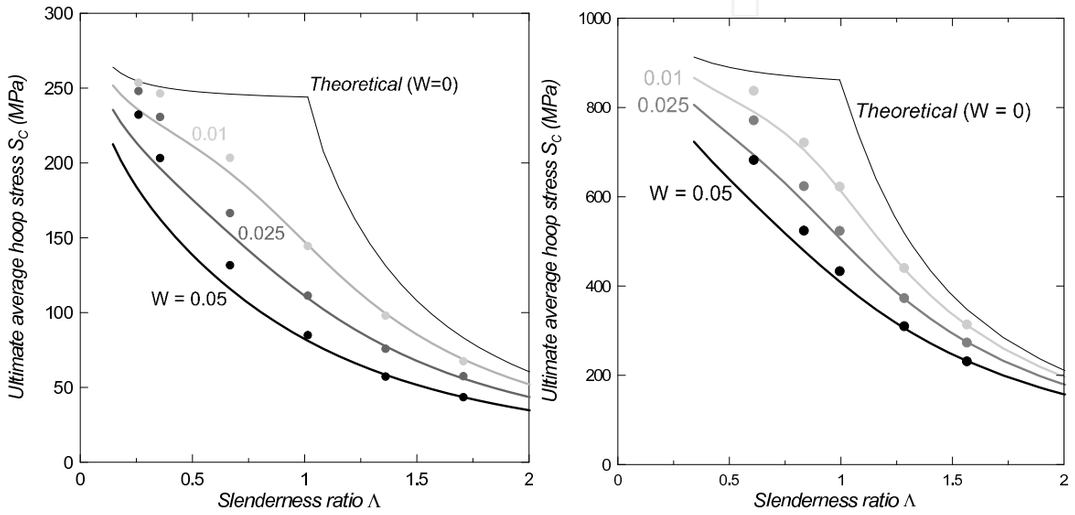

(a) INCONEL 690 ($\kappa = 832$) (b) Titanium alloy ($\kappa = 150$)

Fig. 9. Formula (21) vs computed results (dots). Λ defined by equation (6)

The results provided by equation (21) are plotted in Fig. 9 (solid lines). Dots refer to the results computed in (Corradi et al., 2009), where indication on the assumptions made, the finite element model used and the solution procedure adopted can be found. For graphical purposes, the ultimate pressure is expressed in terms of the average hoop stress equation (2). Agreement is good for $\Lambda > 1$ but, as the thickness increases, lower bounds rather than good approximations are obtained. It can be concluded that thin or moderately thin tubes behave essentially as straight columns of rectangular cross section, but some fundamental aspects of the structural response change drastically as the thickness increases beyond a certain limit.
A first reason for this change is of purely geometric nature, i.e. it depends on the value of D/t only. For comparatively large values the tube wall behaves essentially as a straight column, but curvature increases with diminishing D/t and differences become more and more evident. Secondly, thick tubes exhibit stress redistribution capabilities that columns do not have and this provides additional resources in terms of overall strength. It must be observed that stress redistribution *capability* depends on D/t only, but the possibility of actually exploiting it is conditioned by tube slenderness Λ which, as equation (6) shows, depends on both D/t and the material properties subsumed by the dimensionless parameter κ, equation (8).
Fig. 9 indicates that the second effect is dominant. Because of the strong difference in κ, $\Lambda = 1$ corresponds to $D/t \approx 30$ for INCONEL 690 and to $D/t \approx 13$ for titanium alloy. The two

pictures do show some differences, but not as strong as the discrepancy between the two D/t values would suggest: computed results for titanium depart from formula predictions for a slightly greater Λ than for INCONEL, but the overall response seems to depend more on Λ as a whole than on D/t only.
In any case, equation (21a) provides conservative estimates for the failure pressure of thick tubes. In (Corradi et al., 2008) this result was considered effectively as a *lower bound* and a corresponding upper bound, consisting in the plastic collapse load of the ovalized tube computed by neglecting geometry changes, was associated to it. The two bounds were combined by introducing a suitable weighting factor, determined by fitting a number of computed results for tubes of different materials (including those listed in Table 1). As it was already mentioned, the procedure produced acceptable results, but it is felt that it could be both simplified and improved.

4. The proposed procedure

Both equations (17) for columns and (21) for cylindrical shells predict that the failure pressure coincides with the theoretical limit when the relevant parameter Z vanishes. This obviously occurs for any slenderness ratio when no imperfections are present ($W = 0$) but, independently of the presence of imperfections, both structures are expected to become stocky enough to make negligible interaction with buckling. In other words, it should be $Z = 0$ for any W when slenderness attains a sufficiently low value.
Equation (17b) in fact implies $Z \to 0$ for $\Lambda \to 0$, so that one obtains $P_C = N_0$ for infinitely stocky columns, independently of the imperfection amplitude. However, to give $Z = 0$ for $W \neq 0$, equation (21b) requires $\frac{D}{t} = -\frac{1}{2}$, a value with no physical meaning. This is another reason for the increasingly conservative nature of the approximation as Λ diminishes.
The remarks above suggest that the approximation can be improved by operating on the expression (21b) of Z so to make it vanish for sufficiently small D/t. A minimal choice is $D/t = 2$, the lowest possible value, which however turns out to be still too restrictive. Moreover, the discussion in the preceding section shows that, to obtain an approximation reasonably accurate for all materials, slenderness ratio Λ is preferable to D/t as a measure of the limit stockiness. On the basis of the numerical results in (Corradi et al., 2009), this can be reasonably identified with $\Lambda = 0.2$ and the corresponding values of D/t for different materials can be obtained by numerically solving equation (6). For the materials considered in Table 1, the resulting values, labeled as $(D/t)_{\Lambda=0.2}$, are listed in the last column.
The correction consists in replacing the term $(D/t + 1/2)$ with $(D/t - (D/t)_{\Lambda=0.2})$ in equation (21b). This improves the approximation for $\Lambda < 1$, but shifts the curves upward everywhere by an amount of some significance, even if not dramatic and diminishing with increasing Λ. For compensation, the imperfection amplitude is artificially increased by multiplying W by a factor that, empirically, was identified with 1.2. Thus, the expression for Z becomes

$$Z = \frac{\sqrt{3}}{2}\left(\frac{D}{t} - \left(\frac{D}{t}\right)_{\Lambda=0.2}\right) 1.2\, W \tag{22}$$

If equation (21b) is replaced by the expression above, equation (21a) produces the results depicted in Fig. 10 for the four materials listed in Table 1, covering a range of values of κ that can be regarded as exhaustive. Plots depart from the value of Λ corresponding to $D/t = 5$, which is different for different materials. Formula predictions show a very good agreement throughout with numerical results (dots). For materials with low values of κ (aluminum and

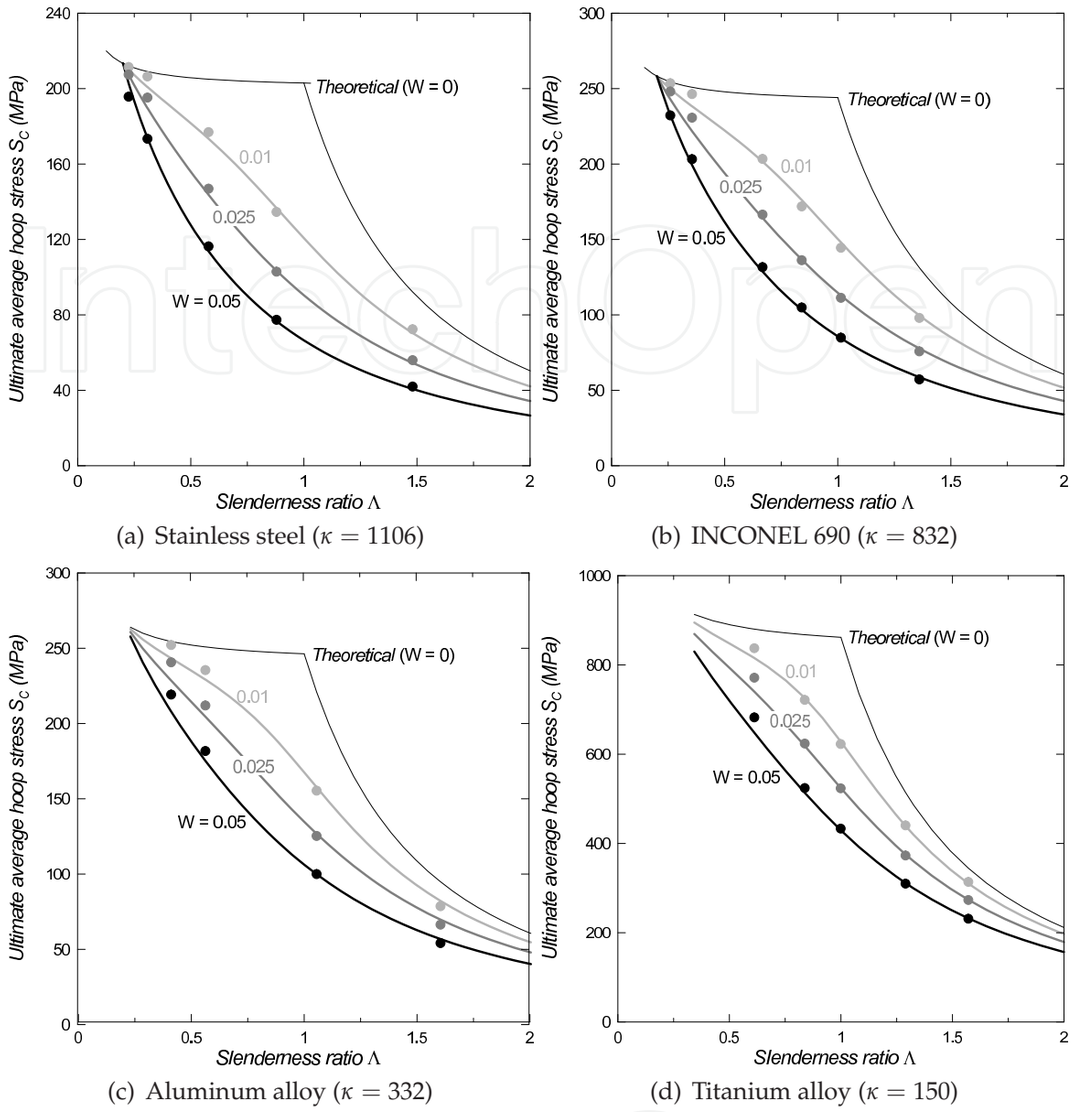

(a) Stainless steel ($\kappa = 1106$) (b) INCONEL 690 ($\kappa = 832$)

(c) Aluminum alloy ($\kappa = 332$) (d) Titanium alloy ($\kappa = 150$)

Fig. 10. Proposed formula vs computed results. Λ defined by equation (6)

titanium alloys) they remain a little conservative for stocky tubes, but improvement with respect to the unbridged formula is significant.

5. Shortcomings of thin shell approximation

In the formula above the theoretical limit values are defined by equations (1) and, as a consequence, the slenderness ratio by equation (6). Use of these expressions is mandatory in a context that includes thick and moderately thick tubes, in that they incorporate the effects of stress redistribution over the wall thickness, which were seen to be significant and which the "thin shell" equations (4), (7) ignore. Nevertheless, the latter expressions often are preferred and the implications of their use are worth exploring.

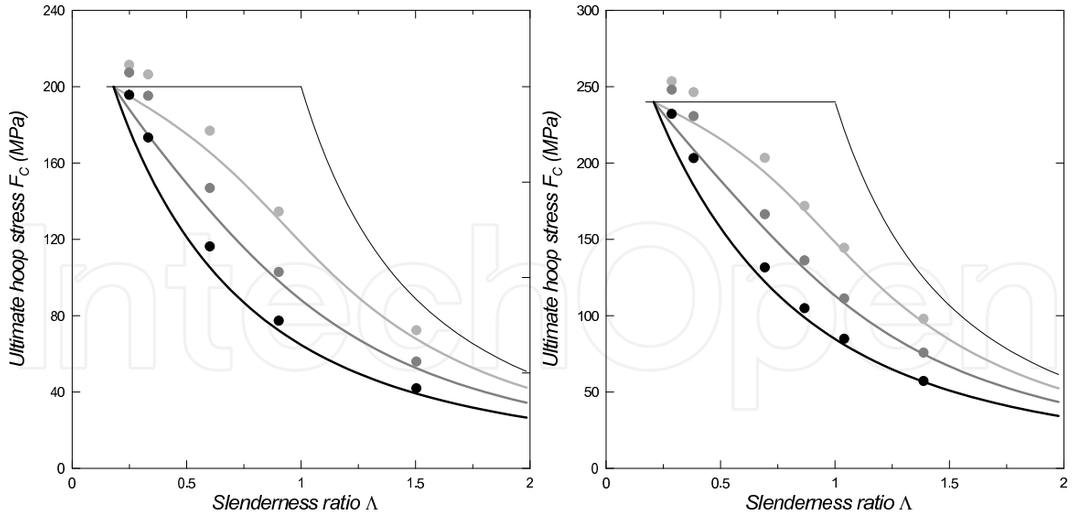

(a) Stainless steel ($\kappa = 1106$)

(b) INCONEL 690 ($\kappa = 832$)

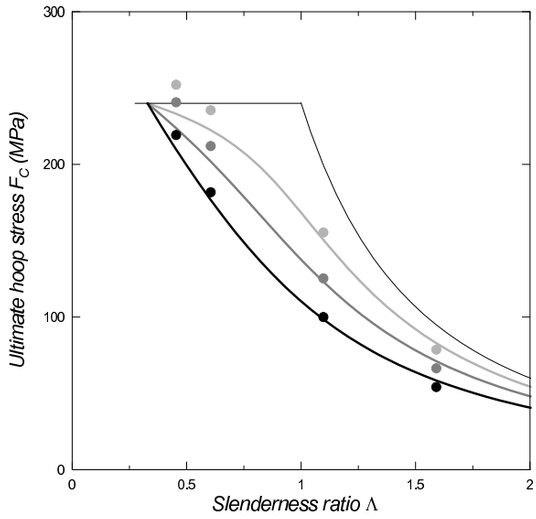

(c) Aluminum alloy ($\kappa = 332$)

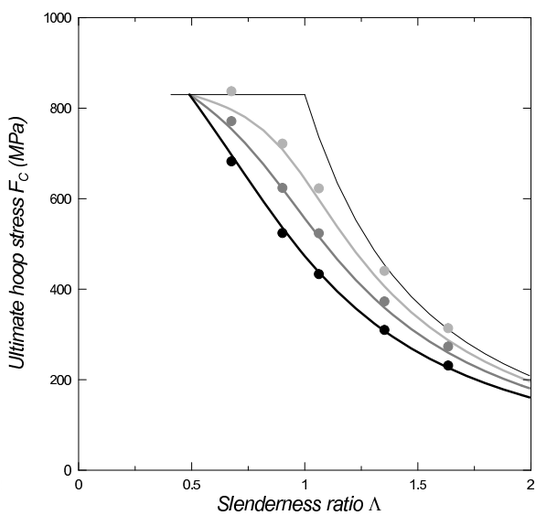

(d) Titanium alloy ($\kappa = 150$)

Fig. 11. Results obtained with thin shell approximation. Λ defined by equation (7)

Formally, modifications are straightforward. It suffices to replace in equation (21a) q_0 and q_E with p_0 and p_E, as defined by equations (4). One obtains

$$p_C = \frac{1}{2}\left[p_0 + p_E\,(1+Z) - \sqrt{(p_0 + p_E\,(1+Z))^2 - 4p_0p_E}\right] \tag{23a}$$

The value of Z still could be given by equation (22), whith $(D/t)_{\Lambda=0.2}$ computed from equation (7). However, the choice for a limiting value of D/t associated to a material independent slenderness ratio is justified by the dominant effect of stress redistribution, associated with Λ. Thin shell approximation does not account for stress redistribution and the only cause of departure of the tube response from that of the straight column is the geometric curvature, so that a limiting value of D/t seems the most appropriate choice. An acceptable

compromise, valid for all materials, turns out to be $(D/t)_{\lim} = 6$ and one can write

$$Z = \frac{\sqrt{3}}{2}\left(\frac{D}{t} - 6\right) 1.2\, W \tag{23b}$$

The results provided by equations (23a) are depicted in Fig. 11. Results are not as accurate as those in Fig. 10, but still acceptable in the moderately thin and thin tube range. As well expected, predictions become grossly conservative with increasing thickness, which underlines the importance of properly accounting for stress redistribution. To assess the pressure bearing capacity of the tube, thin shell theory is adequate only to more than moderately thin tubes (i.e., thinner than those for which an elastic solution still is acceptable) and a formulation aiming at covering the entire slenderness range must consider more precise expressions. One cannot even claim that these shortcomings are compensated by greater simplicity: equations (23a) are not simpler; only they are based on more usual definitions.

6. Conclusions

Long cylindrical shells subjected to external pressure have been considered. The study was motivated by the necessity of assessing the collapse behavior of the moderately thick tubes involved by some recent nuclear power plant proposals, but tubes of any slenderness were considered, even if little attention was devoted to very thin tubes, which buckle when still elastic according to well known modalities and that do not need additional investigation.
In previous papers it was demonstrated that a reliable reference value for the pressure causing tube failure can be obtained by performing complete non linear finite element computations under suitable assumptions. Purpose of this study was the derivation of an accurate and simple formula permitting the definition of this value without performing numerical analyses. It does not seem too daring to state that this goal has been attained with equations (21a), (22): the formula is fairly simple and the results it provides are in good agreement with numerical outputs for different materials, imperfection amplitudes and slenderness ratios. Obviously, only a few materials, imperfections and slendernesses have been checked, but the range of parameters used is wide enough for this statement to be considered of general validity.
The formula can be used both for preliminary design purposes and as a reliable reference value for the definition of allowable working pressure. This second aspect, however, no longer is a must: since Code Case N-759 was approved, tubes can be sized adequately by using existing regulations and alternatives are not required. In the authors' opinion, however, this fact does not diminish the interest of the result achieved. The ingredients used to build the formula enlighten some aspects of the collapse behavior of moderately thick tubes, a range so far little explored. Tubes of intermediate slenderness fail because of interaction between buckling and plasticity, but differences show up at slendernesses about the transition value. Medium thin tubes behave essentially as straight columns and column formulas can be employed with straightforward modifications. As thickness increases, however, the geometry dependent effect of curvature and the slenderness dependent effect of stress redistribution enter the picture and the tube wall no longer behaves as a straight beam. To account for these aspects, a correction was introduced to the original formula. The accuracy of the consequent results can be taken as the indication that the fundamental aspects of the mechanical behavior are correctly represented.

7. Acknowledgment

Authors express their gratitude to Mr Giovanni Costantino and Mr Manuele Aufiero for performing some of the computations used in this study.

8. References

ASME (2007). Code Case N-759: Alternative rules for determining allowable external pressure and compressive stresses for cylinders, cones, spheres and formed heads, In: *BPVC-CC-N-2007 Nuclear Code Cases; Nuclear components*, ASME International, 2007. ISBN 0791830764.

Budiansky B. (1974). Theory of buckling and post-buckling behaviour of elastic structures. *Advances in Applied Mechanics*, Vol. 14, Issue C, 1974, 1-65, ISSN 0065-2156.

Carelli M.D.; Conway L.E.; Oriani L.; Petrovic B.; Lombardi C.V.; Ricotti M.E.; Baroso A.C.O.; Collado J.M.; Cinotti L.; Todreas N.E.; Grgic D.; Moraes M.M.; Boroughs R.D.; Ninokata H.; Ingersoll D.T. & Oriolo F. (2004). The design and safety features of the IRIS reactor. *Nuclear Engineering and Design*, Vol. 230, No. 1-3, May 2004, 151-167, ISSN 0029-5493.

Carelli M.D. (2009). The exciting journey of designing an advanced reactor. *Nuclear Engineering and Design*, Vol. 239, No. 5, May 2009, 880-887, ISSN 0029-5493.

Cinotti L.; Bruzzone M.; Meda N.; Corsini G.; Lombardi C.V.; Ricotti M. & Conway L.E. (2002). Steam generator of the International Reactor Innovative and Secure, *Proceedings of the Tenth International Conference on Nuclear Engineering (ICONE)*, Arlington, VA, Paper No. ICONE10-22570.

Corradi L.; Luzzi L. & Trudi F. (2005). Collapse of thick cylinders under radial pressure and axial load. *ASME Journal of Applied Mechanics*, Vol. 72, No. 4, July 2005, 564-569, ISSN 0021-8936 .

Corradi L.; Ghielmetti C. & Luzzi L. (2008). Collapse of thick tubes pressurized from outside: an accurate predictive formula. *ASME Journal of Pressure Vessel Technology*, Vol. 130, No. 2, May 2008, Paper 021204_1-9, ISSN 0094-9930.

Corradi L.; Di Marcello V.; Luzzi L. & Trudi F. (2009). A numerical assessment of the load bearing capacity of externally pressurized moderately thick tubes. *International Journal of Pressure Vessels and Piping*, Vol. 86, No. 8, August 2009, 525-532, ISSN 0308-0161.

Dowling P.J. (1990). New directions in European structural steel design, *Journal of Constructional Steel Research*, Vol. 17, No. 1-2, July 1990, 113-140, ISSN 0143-974X.

EUROCODE 3 (1993). Design of Steel Structures. Part 1.1: General Rules and Rules for Building, ENV 1-1, Brussels, 1993.

Haagsma S.C. & Schaap D. (1981). Collapse resistance of submarine pipelines studied. *Oil & Gas Journal*, No. 2, February 1981, 86-91, ISSN 0030 1388.

IAEA (2007). *Status of Small Reactor Designs without Onsite Refueling*, International Atomic Energy Agency, IAEA-TECDOC-1536, ISSN 1011-4289.

Ingersoll D.T. (2009). Deliberately small reactors and the second nuclear era, *Progress in Nuclear Engineering*, Vol. 51, No. 4-5, May-July 2009, 589-603, ISSN 0149-1970.

Karahan A. (2010). Possible design improvements and a high power density fuel design for integral type small modular pressurized water reactors, *Nuclear Engineering and Design*, Vol. 240, No. 10, October 2010, 2812-2819, ISSN 0029-5493.

Lo Frano R. & Forasassi G. (2009). Experimental evidence of imperfection influence on the buckling of thin cylindrical shells under uniform external pressure. *Nuclear Engineering and Design*, Vol. 239, No. 2, February 2009, 193-200, ISSN 0029-5493.

Luzzi L. & Di Marcello V. (2011). Collapse of nuclear reactor SG tubes pressurized from outside: the influence of imperfections. *ASME Journal of Pressure Vessel Technology*, Vol. 133, No. 1, February 2011, Paper 011206_1-6, February 2011, ISSN 0094-9930.

Mendelson A. (1968). *Plasticity: Theory and Applications*, McMillan, New York.

Ninokata H. (2006). A comparative overwiev of the thermal hydraulic characteristics of integrated primary systems nuclear reactors, *Nuclear Engineering and Technology*, Vol. 38, No. 1, February 2006, 33-44, ISSN 1738-5733.

Tamano T.; Mimaki T. & Yanagimoto S. (1985). A new empirical formula for collapse resistance of commercial casing, *Nippon Steel Technical Report*, No. 26, 1985, 19-26, ISSN 0300 306X.

Timoshenko S. & Gere J.M. (1961). *Theory of Elastic Stability*, McGraw-Hill, New York.

Timoshenko S. & Goodier J.N. (1951). *Theory of Elasticity*, McGraw-Hill, New York.

Yeh M.H. & Kyriakides S. (1988). Collapse of deepwater pipelines. *ASME Journal of Energy Resources Technology*, Vol. 110, No. 1, March 1988, 1-11, ISSN 0195-8954.

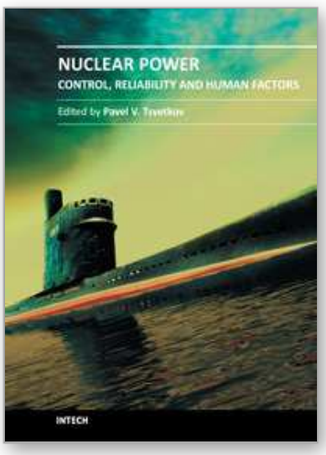

Nuclear Power - Control, Reliability and Human Factors
Edited by Dr. Pavel Tsvetkov

ISBN 978-953-307-599-0
Hard cover, 428 pages
Publisher InTech
Published online 26, September, 2011
Published in print edition September, 2011

Advances in reactor designs, materials and human-machine interfaces guarantee safety and reliability of emerging reactor technologies, eliminating possibilities for high-consequence human errors as those which have occurred in the past. New instrumentation and control technologies based in digital systems, novel sensors and measurement approaches facilitate safety, reliability and economic competitiveness of nuclear power options. Autonomous operation scenarios are becoming increasingly popular to consider for small modular systems. This book belongs to a series of books on nuclear power published by InTech. It consists of four major sections and contains twenty-one chapters on topics from key subject areas pertinent to instrumentation and control, operation reliability, system aging and human-machine interfaces. The book targets a broad potential readership group - students, researchers and specialists in the field - who are interested in learning about nuclear power.

InTech Europe
University Campus STeP Ri
Slavka Krautzeka 83/A
51000 Rijeka, Croatia
Phone: +385 (51) 770 447
Fax: +385 (51) 686 166
www.intechopen.com

InTech China
Unit 405, Office Block, Hotel Equatorial Shanghai
No.65, Yan An Road (West), Shanghai, 200040, China
中国上海市延安西路65号上海国际贵都大饭店办公楼405单元
Phone: +86-21-62489820
Fax: +86-21-62489821

IntechOpen